An alternative and cost-effective biosorbent derived from napier grass stem for malachite green removal

W. Tongpoothorn[1*], O. Somsimee [1], T. Somboon[1], M. Sriuttha[2]

[1]*Department of Chemistry, Faculty of Engineering, Rajamangala University of Technology Isan, Khon Kaen Campus, Khon Kaen, 40000, Thailand.*
[2]*Department of Chemistry, Faculty of Applied Science and Engineering, Khon Kaen University, Nong Khai Campus, Nong Khai, 43000, Thailand.*

Abstract

This work presents an alternative cellulosic biosorbent derived from napier grass stem (NGS) for removing malachite green (MG) from aqueous solution. NGS is modified by a simple process with less reagent usage and low energy required. The removal condition including contact time, initial dye concentration and biosorbent dosage on the adsorption capacity were optimized by using response surface methodology (RSM). The results show that the maximum adsorption capacity of modified NGS (mNGS) was 32.27 mg g^{-1} with contact time of 90 min, initial dye concentration of 100 mg L^{-1} and biosorbent dosage of 0.05 g. The pseudo second order kinetic model and Langmuir isotherm model were best described the adsorption. It was indicated that the adsorption process take place on localized sites without interaction between dye molecules and a saturated monolayer. Thermodynamic study illustrated that the adsorption was physical in nature, endothermic and spontaneous. The results indicate that mNGS could be employed as an alternative and economical biosorbent for removal of MG from aqueous solution.

1. Introduction

Recently, industrial effluents are one of the major causes of environmental pollution. Especially, effluents discharged from dyeing industries which contain large quantities of suspended organic solid. It is not only undesirable, but it also retards light penetration [1]. Malachite green (MG) is a common basic dye used in numerous industries for dyeing, i.e., silk, leather, plastics, paper and others [2, 3]. Moreover, it is extensively used as an antiparasitic and antifungal agent in aquaristics. Both MG and its major metabolites, leucomalachite green (LMG) cause mutagenetic, carcinogenic and teratonic effects to human [4]. Due to its complex molecular structure, this dye is very difficult to be biodegraded and hardly eliminated under natural aquatic environment [5]. Therefore, the dispose of this dye from the effluent before being discharged into the waterways is a management serious concern. Various methods are available for the treatment of MG in effluent such as membrane filter [6], ion exchange [7], chemical coagulation [8] and flocculation [9]. However, the major disadvantage of these method includes expensive operation cost, limited modification and low adaptability for large scale applications. Adsorption has been extensively used for removal of dyes from effluent since it provides cost-effectiveness, high removal efficiency, easy operation and minimal sludge generation. Nowadays, the adsorption of MG on many cellulosic biosorbents has been reported such as coconut coir activated carbon [10], waste pea shell [11], potato leave powder [12], peroxide treated rice husk [13], wood apple shell [14], *A.squmosa* [15], rice husk [16] and pomegranate peel [17]. Although these biosorbents effectively adsorb MG dyes, such plants take a long time to grow as well as many steps and large amounts of chemical reagents and energy in biosorbent preparation are required that restrict their application for dye treatment. Therefore, the fast growing biomaterial with less step and eco-friendly preparation of biosorbents becomes an interested topic. In Thailand, napier grass (NG) or *Pennisetum purpureum* has been promoted for planting to be use as alternative animal feeding. It was attended because of its fast growth without much nutrients supply, good disease resistance, adaptability, high production yield and easy

Tongpoothorn et al., J. Mater. Environ. Sci., 2019, 10 (8), pp. 685-695

685

propagation [18]. NG is also considered as a cheap cellulosic resource. Moreover, it has high biomass production of about 87 t/ha/year with great ability to be harvested five to six times per year [19]. Importantly, NG contains high amount of cellulose content about 35–50% [20]. Thus, this material has been the principal reasons for supplement as an alternative and potential sustainable resource of precursors to produce biosorbent.

To the best of our knowledge, there have been no reports on the utilization of NGS based biosorbent for dye removal. Herein, we present for the first time the efficient of MG dye in aqueous solution by the modified napier grass stem (mNGS) via adsorption process. The optimum conditions for MG adsorption were determined by applying an effective experimental design method, response surface methodology (RSM), based on Box-Benhken design to obtain the highest adsorption capacity and evaluate the influence of independent variables and their interactive effects on responses with a reduced number of experiments [21]. Also, the effect of independent variables including contact time, initial dye concentration and biosorbent dosage on adsorption capacity was determined. Additionally, kinetic, isotherm and thermodynamic studies were studied and reported.

2. Material and Methods
2.1. Materials
Napier grass stem (NGS) used in this study was collected from Bureau of Animal Nutrition Development in Khon Kaen province, Thailand. Malachite green (MG; $C_{23}H_{25}N_2$; 392.02 g mol^{-1}) with 90% purity was purchased from Dy Star Co. (Germany). Its structure and physico-chemical properties are shown in Figure 1. The stock solution of 500.00 mg L^{-1} was prepared by dissolving an appropriate amount of MG dye in deionized water. The working solutions of dyes were prepared by a dilution of the dye stock solution.
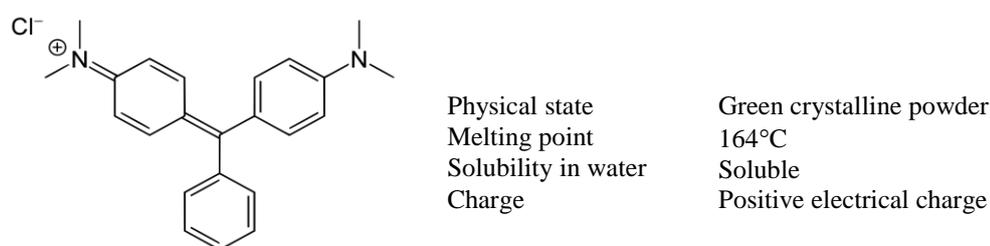

Physical state	Green crystalline powder
Melting point	164°C
Solubility in water	Soluble
Charge	Positive electrical charge

Figure 1: Chemical structure and physico-chemical propteries of malachite green dye

2.2. Preparation of biosorbent
Biosorbent was prepared by simple process with less chemical and energy required. Briefly, NGS was cut, blended and sieved to obtain particle size about 1.4-2.0 mm. Then, it was dried in oven at 80°C. After that, it was mixed with 1.0 M NaOH solution and autoclaved at 121°C at 15 psi for 15 min. The mixture was filtered and washed many times with distilled water until the filtrate was neutral. The residue was dried at 80°C for 24 h and sieved. Consequently, biosorbent which defined as modified NGS (mNGS) was obtained. The overall steps for preparation of mNGS biosorbent are presented in Figure 2.

Figure 2: Schematic for biosorbent preparation.

2.3. Characterization of biosorbent
In order to determine the surface and average pore size of biosorbent, the BET analysis was applied to mNGS using a surface area and pore size analyser (BELSORP, mini-II nitrogen adsorptometer, MicrotracBEL, Japan).

To study the surface functional groups, mNGS before and after dye adsorption was investigated by using attenuated total reflectance fourier transform infrared spectrophotometer (ATR-FTIR, Bruker Tenser 27 spectrophotometer, Ettlingen Co, LTD, Germany) recorded in the range of 4000-650 cm^{-1} whereas the morphology of biosorbent was determined by the scanning electron microscope (SEM, Hitachi TM3030, Japan).

2.4. Batch experiments

Batch experiments designed by RSM were conducted by mixing a certain amount of mNGS with 20.00 mL of dye solution in a 250 mL bottle under an optimum pH value of 5, which related to the results from earlier studies [22, 23]. The mixtures were then immersed in water bath at 45°C with varying contact time, initial dye concentration and adsorbent dosage. After adsorption, the solution was centrifuged and the remaining dye concentration in the solution was analyzed by UV-VIS spectrophotometer (Jasco V530, JASCO International Co, LTD., Japan) at the maximum adsorption wavelength (λ_{max}=616 nm). The total MG dye uptake was calculated from the mass balance equation as follows equation (1):

$$q_e = \left(\frac{C_0 - C_e}{W} \right) \times V \tag{1}$$

where q_e is the adsorption capacity (mg g^{-1}), C_0 and C_e are initial and equilibrium concentrations of MG solution (mg L^{-1}), respectively. V is the volume of the batch solution (L), and W is the amount of the biosorbent (g) used in the experiments.

2.5 Design of experiment for optimization

The experiments were performed using RSM with a Box-Behnken design in order to obtain the maximum adsorption capacity. The three critical parameters affecting MG removal, namely contact time (A), initial dye concentration (B) and biosorbent dosage (C) were chosen as independent variables with 20.00 mL of dye solution. The adsorption capacity was considered as the response. It consists of 17 experiments that are designed by Design Expert software (version 7.0.0, Stat. Ease. Inc, United States) statistical package. For the optimization process, the response can be simply related to the chosen factors, by linear model and is given below and designated equation (2):

$$Y = \beta_0 + \beta_1 A + \beta_2 B + \beta_3 C + \beta_{12} AB + \beta_{13} AC + \beta_{23} BC + \beta_{11} A^2 + \beta_{22} B^2 + \beta_{33} C^2 \tag{2}$$

where Y is the process response (adsorption capacity) and A, B and C represent the effect of the independent variables. Thus, A^2, B^2 and C^2 are the square effects and AB, AC and BC are the interaction effects, β_0 is the regression coefficient at center point, β_1, β_2 and β_3 are linear coefficients, β_{12}, β_{23} and β_{13} are the interaction coefficients and β_{11}, β_{22} and β_{33} are quadratic coefficients. The adequacy of the proposed model is then exhibited using the diagnostic checking tests provided by analysis of variance (ANOVA). The optimum values of the parameters were examined by solving the regression equation, analyzing the surface of the 3D and contour plots.

2.6 Adsorption studies

Kinetic adsorption is conducted to investigate the mechanism of adsorption and determine equilibrium time. For this purpose, 0.05 g of biosorbent was mixed with 20.00 mL of dye solution with initial concentration of 100 mg L^{-1}. Then it was immerged in water bath at 45°C for different time intervals. After that the adsorbent was separated by centrifugation. The residual dye concentration was analyzed by UV-VIS spectrophotometer.

Adsorption isotherms are used to describe the equilibrium behaviors of MG uptake. The equilibrium experiments were carried out under constant temperature of 45°C for 90 min of contact time, whereas the initial concentration was varied in the range of 10-100 mg L^{-1}. After this period, the solution was centrifuged. The remaining dye concentration was analyzed. The adsorption equilibrium data were explained by Langmuir and Freudlich isotherms, which are the most widely used for describing the interaction between adsorbate and adsorbent. Thermodynamic parameters are important in adsorption studies for better understanding of the effect of temperature on adsorption. It was carried out at different temperatures (25, 35, 45 and 55°C). Experiments were performed with 20.00 mL of 100 mg L^{-1} dye solution and constant biosorbent dosage of 0.05 g. The samples were immerged in water bath for 90 min. The experimental values obtained were evaluated for the thermodynamic parameters.

3. Results and discussion

3.1 Characterization of the biosorbent

ATR-FTIR spectra of mNGS before and after MG adsorption are shown in Figure 3. It was observed that both spectra exhibited a broad and intense band around 3333 cm^{-1} corresponding to the -OH stretching vibration [18]. Band at 2892 cm^{-1} was assigned to stretching vibration of –CH$_2$- of cellulose, hemicellulose and lignin constituents [24]. The band at 1638 cm^{-1} indicated the presence of C=O stretching in carbonyl and carboxyl group [25]. The band around 1425 cm^{-1} related to C=C in aromatic compound. The absorption bands at 1366 and 1317 cm^{-1} corresponded to C-H asymmetric deformation and –OH bending vibration of cellulose, respectively [26]. Peak at 1262 cm^{-1} was assigned to COO- vibration of acetyl group in hemicellulose [24]. Another absorption band around 1029 cm^{-1} was attributed to the C-O stretching. The peak at 896 cm^{-1} indicated the presence of aromatic heterocyclic molecules. However, it was observed that both spectra were quite similar, implying that there was no breaking or creating of chemical bond and the interaction between biosorbent and dye molecule was physisorption. Moreover, SEM photographs of mNGS before MG adsorption showed a rough surface and heterogeneous pores which were a possibility for dye molecule to be trapped and adsorbed, as can be observed that these pores were filled after adsorption of MG. However, by the textural data of mNGS indicated that it has quite low surface area (BET surface area = 4.0525 m^2 g^{-1}), mean pore diameter of 4.8553 nm and total pore volume (p/p_0 = 0.975) of 0.0049191 cm^3 g^{-1}, which implied that the adsorption possibility occurs only on the surface of biosorbent.
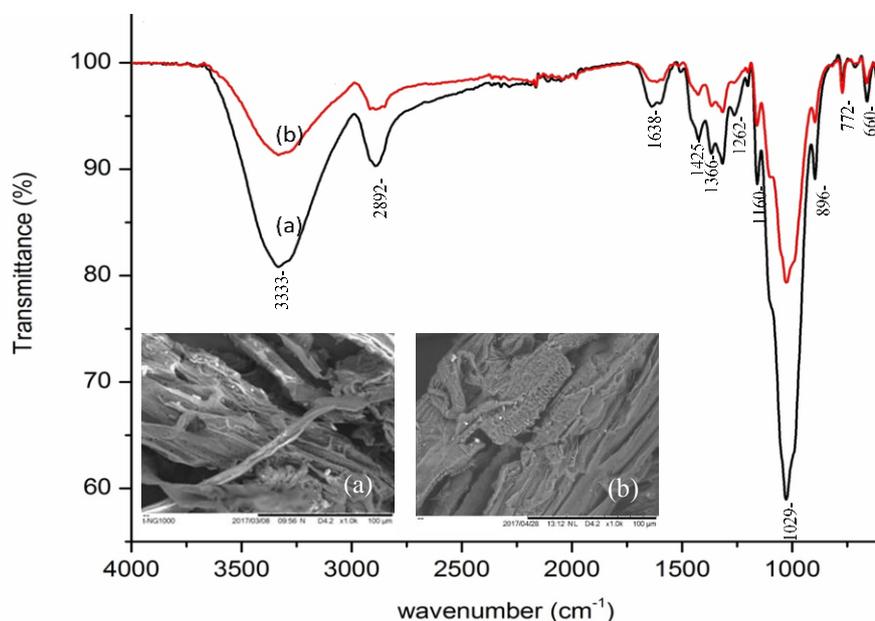

Figure 3 : ATR-FTIR spectra and SEM photographs of mNGS before (a) and after (b) MG adsorption.

3.2 Box-Behnken statistical analysis

A total of 17 runs of Box-Behnken experimental design and the response from experimental runs were calculated from equation (1) and shown in Table 1. The experimental adsorption capacity was found to be in the range of 6.61-32.27 mg g^{-1}. The highest adsorption capacity was obtained at 60 min of contact time, 100 mg L^{-1} MG and 0.05 g of mNGS. Table 2 shows the analysis of variance (ANOVA) of regression parameters of the predicted response surface quadratic model for MG adsorption on mNGS. Based on the results, the response surface model constructed in this study for predicting adsorption capacity was considered reasonably. In terms of actual factors, an empirical relationship between adsorption capacity (Y) and process variable can be expressed by the following second-order polynomial equation in the form of the final equation in terms of code factors as below:

$$Y = +14.8+0.25*A+4.87*B-7.28*C+0.26*A*B-0.21*A*C- 2.24*B*C- 0.29*A^2+0.081*B^2 +2.94*C^2 \quad (3)$$

Positive sign in front of each term indicates synergistic effect, while a negative sign indicates antagonistic effect. The quality of the model developed was evaluated based on the correlation coefficient value [27]. In the present study, the high value of correlation coefficient (R^2=0.9967) and smaller standard deviation were observed indicating that only 0.33% of the total dissimilarity might not be explained by the empirical model. High value of R^2 with the value of adjusted determination coefficient R^2 of 0.9925 illustrates a high degree of correlation between the calculated and observed results within the range of experiment.

Table 1 : Response values for different experimental conditions.

Run	Factor 1 A:contact time (min)	Factor 2 B:initial dye conc. (mg L^{-1})	Factor 3 C:biosorbent dosage (g)	Response Adsorption capacity (mg g^{-1})
1	90	100	0.10	18.94
2	60	75	0.10	14.33
3	90	75	0.15	9.77
4	30	75	0.15	9.78
5	30	75	0.05	23.47
6	90	75	0.05	24.30
7	60	50	0.05	17.12
8	30	100	0.10	17.83
9	90	50	0.10	9.60
10	60	50	0.15	6.61
11	60	75	0.10	14.35
12	30	50	0.10	9.52
13	60	100	0.05	32.27
14	60	100	0.15	12.80
15	60	75	0.10	14.19
16	60	75	0.10	14.02
17	60	75	0.10	14.01

Table 2 : ANOVA for analysis of variance and adequacy of the quadratic model.

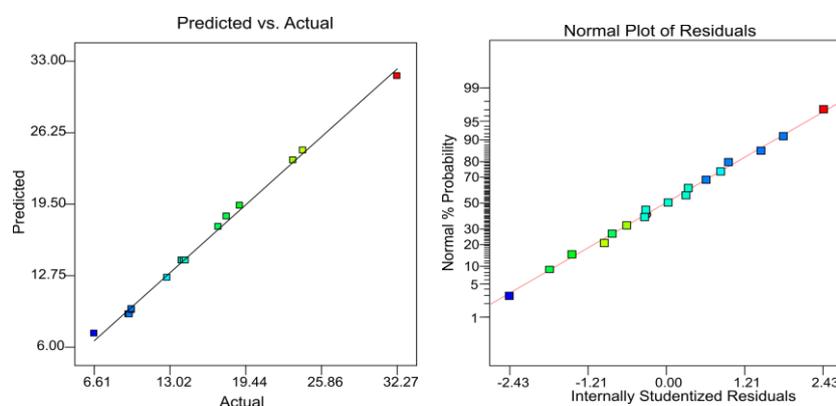| Source	Sum of squares	df	Mean square	F-value	p-value Prove > F
Model	671.27	9	74.59	236.15	< 0.0001
A-time	0.52	1	0.52	1.64	0.2415
B-conc.	190.08	1	190.08	601.82	< 0.0001
C-dosage	423.54	1	423.54	1340.99	< 0.0001
AB	0.26	1	0.26	0.84	0.3902
AC	0.18	1	0.18	0.56	0.4774
BC	20.06	1	20.06	63.53	< 0.0001
A^2	0.35	1	0.35	1.10	0.3293
B^2	0.027	1	0.027	0.087	0.7772
C^2	36.34	1	36.34	115.04	< 0.0001
Residual	2.21	7	0.32		
Lack of fit	2.10	3	0.70	26.17	0.0043
Pure error	0.11	4	0.027		

SD=0.56, PRESS=33.83, R^2=0.9967, R^2_{adj}=0.9925, Adeq Precision=56.379

Figure 4 : Predicted versus actual plot and normal probability plot of the studentized residual for MG adsorption.

Tongpoothorn et al., J. Mater. Environ. Sci., 2019, 10 (8), pp. 685-695

689

Figure 4 further confirms that the predicted values of MG adsorption from the model were in agreement with the actual experimental data as can be seen that the actual values are distributed fairly close to the straight line. Furthermore, the diagnostic plots such as normal probability plot of the studentized residuals was applied to assess the fitted model to ensure that the selected model provides an adequate approximation of the real system. Moreover, a normal probability plot in Figure 4 show that the experiment data is symmetrically arranged within the confidence level and explained the suitability of the quadratic model [28]. From the ANOVA for response surface model for MG adsorption capacity, the large model F-value of 236.15 and p-value (Prove>F) less than 0.05 implied that model terms are significant [29]. In this case, initial dye concentration (B), biosorbent dosage (C), interaction term of BC and quadratic term of C^2 were significant model terms whereas contact time (A), interaction terms (AB and AC) and quadratic terms (A^2, B^2) were all insignificant to the response. The adequate precision measuring the signal to noise ratio of the model was 56.397 (adequate precision > 4), which is an adequate signal for the model [30]. Moreover, low value of %error (SD=0.56) confirmed that the statistical model obtained from this study was both accurate and dependable. The lack of fit F-statistic was significant as the p-values of 26.17 indicated some systematic variation unaccounted for in the hypothesized model. This may due to the exact replicate values of the independent variable in the model that provide an estimate of pure error.

3.3 The optimized conditions and effects of variables on adsorption capacity

To understand the effect of each variable, three dimension (3D) and contour plots were made for the estimated responses, which were the bases of the model polynomial function for analysis, to investigate the significant interactive effect of two variables on the adsorption capacity within the experimental ranges given in Figure 5.
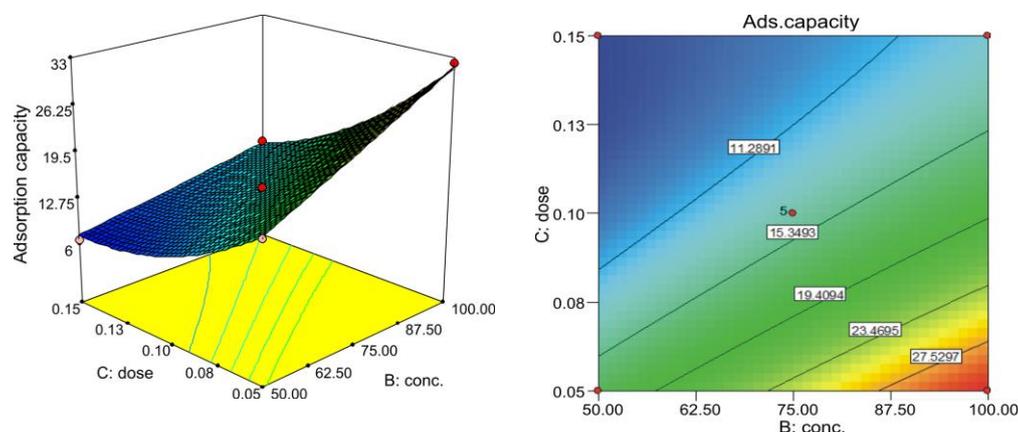

Figure 5 : 3D surface and contour plots for the effect of initial dye concentration and biosorbent dosage on adsorption capacity.

The most effective variable influencing the adsorption of MG on mNGS was biosorbent dosage (C) due to its largest coefficient (as equation 3). The negative sign of this coefficient meant that adsorption capacity was favored at low values of biosorbent dosage due to the limited number of dye molecules. At low biosorbent dosage, the adsorption of dye was quickly and efficiently saturated, whereas at higher biosorbent dosage, more active adsorption sites were available, leading to a lower adsorption capacity [31]. Another variable affecting the response was an initial dye concentration (B). Its coefficient showed a positive sign that indicated an increase in adsorption capacity with increasing the initial dye concentration. This behavior can be attributed to more dye molecules present to be adsorbed onto the surface of the mNGS [32] and an increase of mass transfer driving force between the aqueous and solid phases [33]. Considering the interactive effect of variable, only the interaction between initial dye concentration and biosorbent dosage (BC) showed significant effect on the adsorption capacity. MG adsorption capacity increased when an initial dye concentration increased up until 100 mg L^{-1} but decreased when using more amount of biosorbent dosage. The quadratic effect of variables was not found to be significant for the adsorption capacity, except adsorbent dosage (C^2). Therefore, an optimum condition for MG adsorption on mNGS was 90 min of contact time, 100 mg L^{-1} of initial dye concentration and 0.05 g of mNGS. Under these conditions, the predicted adsorption capacity was 32.03 mg g^{-1} with the desirability of 0.990. It was noticed that the adsorption capacity of mNGS prepared in this work was higher than those of some biosorbents reported in previous works as shown in Table 3. The comparison supported that mNGS prepared from cheap and abundance precursor by simple method with less chemical usage can be promising as an alternative and ecofriendly biosorbent.

Table 3 : Comparison of adsorption capacities with other biosorbents for MG.

Biosorbent	q_m (mg g^{-1})	References
Coconut coir activated carbon	27.44	[11]
Waste pea shell	6.20	[12]
Potato leave powder	33.30	[13]
Peroxide treated rice husk	26.60	[14]
Wood apple shell	34.56	[15]
A.squmosa (CAS)	25.91	[16]
Rice husk	6.50	[17]
Pomegranate	32.47	[18]
mNGS	32.27	This work

3.4 Adsorption study

3.4.1 Kinetic study: in order to explore the mechanisms of MG adsorption on mNGS, the pseudo first order and pseudo second order kinetic models were investigated and expressed as equation (4) and (5), respectively [32]:

$$\frac{1}{q_e} = \frac{k_1}{q_e}\frac{1}{t} + \frac{1}{q_e} \tag{4}$$

$$\frac{t}{q_t} = \frac{1}{k_2 q_2^2} + \frac{t}{q_e} \tag{5}$$

where q_e and q_t are the adsorption capacity (mg g^{-1}) of the adsorbent for dye adsorbed in equilibrium and time (min), respectively, k_1 is the first order rate constant (min^{-1}) and k_2 is the second order rate constant (g mg^{-1}min^{-1}). The results of kinetic studies are presented in Figure 6 and correlation parameters for the adsorption kinetics in the two models are summarized in Table.4. This results indicated that MG adsorption on mNGS fitted the pseudo second order kinetics model well based on the higher correlation coefficient R^2 (1.000) and predicted q_e value was close to the experimental value meaning that the adsorption process may be controlled by multiple factors including adsorbent dosage and initial dye concentration. However, the pseudo second order kinetic model assumes that the adsorption process occurs on localized sites without interaction between the dye molecules and maximum adsorption related to a saturated monolayer of dye molecules onto the mNGS surface. Similar observation and explanation were presented in the research of Keun-Young Shin, et al. [34].
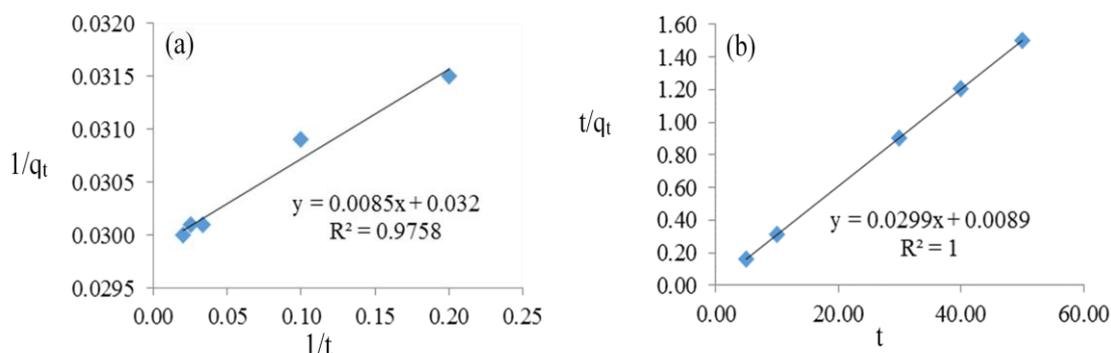

Figure 6 : Pseudo first order (a) and pseudo second order (b) plots.

Table 4 : Pseudo first order and pseudo second order model parameters for MG adsorption.

Pseudo first order			Pseudo second order			$q_{e (exp)}$ (mg g^{-1})
$q_{e (cal)}$ (mg g^{-1})	k_1	R^2	$q_{e (cal)}$ (mg g^{-1})	k_2	R^2	
31.25	0.2428	0.9758	33.44	0.1005	1.000	32.27

3.4.2 Adsorption isotherm study

Several parameters provided by isotherm equilibrium models suggest the surface characteristics of the biosorbent and its adsorption ability, resulting in predicting the maximum equilibrium adsorption capacity. In this work, Langmuir and Freundlich isotherms were studied in order to examine the adsorption mechanism of MG by mNGS. The Langmuir model can be written in the form as shown in Eq. (6) :

$$\frac{1}{q_e} = \frac{1}{q_m} + \frac{1}{q_m k_L}\frac{1}{C_e} \tag{6}$$

where q_m and q_e (mg g^{-1}) are the maximum adsorption and adsorption amount at equilibrium, respectively. C_e (mg L^{-1}) is the concentration of MG at equilibrium; k_L (L mg^{-1}) is the Langmuir constant associated with a saturated monolayer [35]. The Langmuir model describes the monolayer adsorption of MG and the surface of biosorbent. Moreover, one specific site of the adsorbent is filled by only equally sized and shaped of adsorbate without further adsorption by other molecule [35-37]. Thus, the adsorption onto the surface is strongly associated with the driving force and surface area. The Freundlich model, as an exponential equation, assumes that the biosorbent surface is heterogeneous and provides sites with varying affinities [38-39]. This model can predict the occurrence of infinite surface coverage, which is related to multilayer adsorption on the surface. The Freundlich model can be expressed in the form as given in equation (7) :

$$\ln q_e = \ln K_F + \frac{1}{n}\ln C_e \tag{7}$$

where q_e (mg g^{-1}) is the adsorption amount at equilibrium, and C_e (mg L^{-1}) is the concentration of MG at equilibrium; K_F (mg^{1-n}. L^n g^{-1}) and n are the Freundlich constant associated, which are closely related to the adsorption capacity and a nonlinear index related to adsorption intensity, respectively. The results are shown in Figure 7.
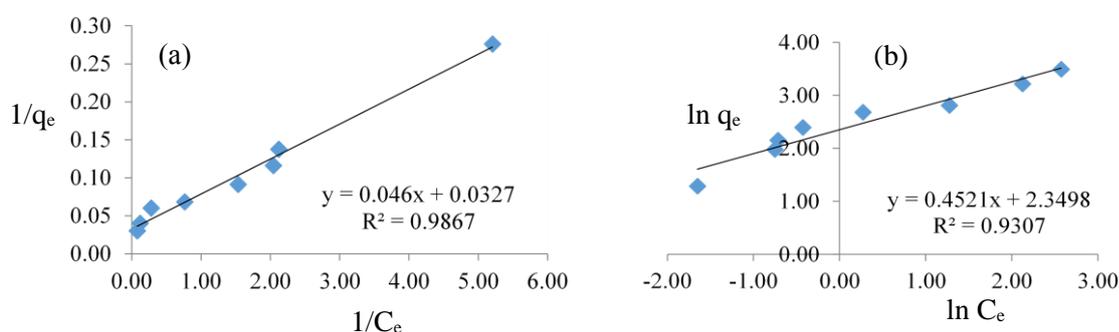

Figure 7 : Langmuir (a) and Freundlich (b) adsorption isotherms.

According to the calculated parameter as shown in Table 5, it was observed that the Langmuir model was more suitable for describing the adsorption process than the Freundlich model based on R^2 close to unity. Moreover, the value of Freundlich parameter (n=2.21) of this study is higher unity, indicating a physical process with mainly monolayer adsorption of MG onto mNGS [40].

Table 5 : Langmuir and Freundlich isotherm parameters for the adsorption of MG.

Langmuir isotherm			Freundlich isotherm		
q_m (mg g^{-1})	K_L (L mg^{-1})	R^2	K_F (mg g^{-1})(L mg^{-1})$^{1/n}$	n	R^2
30.5810	0.7109	0.9867	0.8543	2.21	0.9307

3.4.3 Thermodynamic study

Thermodynamic parameters such as Gibbs free energy ($\Delta G°$, kJ mol^{-1}), enthalpy change ($\Delta H°$, kJ mol^{-1}) and entropy change ($\Delta S°$, kJ mol^{-1}) were calculated using the following relationships as shown in equation (8) and (9)

Tongpoothorn et al., J. Mater. Environ. Sci., 2019, 10 (8), pp. 685-695

692

$$\ln K_D = -\frac{\Delta H^O}{RT} + \frac{\Delta S^O}{R} \tag{8}$$

$$\Delta G^o = \Delta H^o - T\Delta S^o \tag{9}$$

K_D is the equilibrium adsorption distribution constant, R is the gas constant (8.314 J mol K^{-1}) and T is the absolute temperature (K) [41]. From Table 6, the positive value of ΔH° (+19.7618 kJ mol^{-1}) suggested that adsorption process was endothermic in nature. Moreover, based on the values of the enthalpy change for physical adsorption (2.1-20.9 kJ mol^{-1}) and chemical adsorption (80-200 kJ mol^{-1}) [42], the adsorption of MG onto mNGS was considered as physical process. The positive value of ΔS° (+0.0752 kJ mol^{-1}) indicated an increased randomness at the solid/solution interface during the adsorption of MG onto mNGS [22]. Additionally, the negative value of ΔG° illustrated that MG adsorption was a spontaneous and feasible process. These values decreased with an increase in the temperature from 25 to 55°C, implying that the adsorption was more favorable at higher temperature. Similar results were reported for removal of MG from aqueous solution using degreased coffee bean [22].

Table 6 : Thermodynamic parameters for MG adsorption onto mNGS.

ΔH° (kJ mol^{-1})	ΔS° (kJ mol^{-1})	ΔG° (kJ mol^{-1})			
		25°C	35°C	45°C	55°C
+19.7618	+0.0752	-2.6478	-3.3998	-4.1518	-4.9038

3.5 Mechanism of MG dye adsorbed on mNGS

mNGS consisted mainly of cellulose, hemicellulose, lignin and extractives that show the presence of carboxyl, hydroxyl and carbonyl groups in their structure. Consequently, these groups may provide the binding of the cationic dye molecules to the surface of the adsorbent. In addition, the presence of lone pair electrons on oxygen atoms of the functional groups enhances the acumination of the electron deficient positively changed dye molecules, promoting the adsorption. Therefore, the possible adsorption mechanism of MG dye on mNGS would be involved with the electrostatic interaction between the cationic of MG dye and the anionic surface of mNGS.

Conclusion

In summary, the best fit model and the optimization of all variables are successful done through the BBD of the RSM with satisfactory precision and reliability of the experiments. The adsorption of MG on mNGS strongly depends on initial dye concentration and biosorbent dosage. The maximum adsorption capacity is determined to be 32.27 mg g^{-1}, which corresponds to the predicted value of 32.03 mg g^{-1}. Based on the determination coefficient, modeling equilibrium sorption data pointed out that the results are in good agreement with pseudo second order kinetic model. The results indicate that the adsorption process is controlled by both initial dye concentration and biosorbent dosage with no collaboration of dye molecules. The corresponding adsorption isotherm is Langmuir model, describing a monolayer behavior. The adsorption of of MG onto the mNGS is an endothermic and spontaneous process. The mechanism of MG dye adsorbed on mNGS occurs through a physical adsorption process via electrostatic interaction. Based on the results, it is concluded that mNGS can be promised as a potential low cost, easily available and environment friendly biosorbent for MG removal. Additionally, it may also be effective in removing other toxic dyes or heavy metals contaminants in the wastewater.

References
1. J.H. Sun, S.P. Sun, G.L. Wang, L.P. Qiao, Degradation of azo dye Amido black 10B in aqueous solution by Fenton oxidation process, *Dyes Pigm.,* 74 (2007) 647-652. https://doi.org/10.1016/j.dyepig.2006.04.006
2. F. Nekouei, H. Noorizadeh, S. Nekouei, M. Asif, I. Tyagi, S. Agarwal, V.K. Gupta, Removal of malachite green from aqueous solutions by cuprous iodide–cupric oxide nano-composite loaded on activated carbon as a new sorbent for solid phase extraction: Isotherm, kinetics and thermodynamic studies, *J. Mol. Liq.,* 213

(2016) 360-368. https://doi.org/10.1016/j.molliq.2015.07.058

3. R. Gong, X. Zhang, H. Liu, Y. Sun, B. Liu, Uptake of cationic dyes from aqueous solution by biosorption onto granular kohlrabi peel, *Bioresour. Technol.,* 98(6) (2007) 1319-1323. https://doi.org/10.1016/j.biortech.2006.04.034

4. S. Srivastava, R. Sinha, D. Roy, Toxicological effects of malachite green, *Aquat. Toxicol.,* 66 (2004) 319-329. https://doi.org/10.1016/j.aquatox.2003.09.008

5. A. Kar, Y.R. Smith, V. Subramanian, Improved photocatalytic degradation of textile dye using titanium dioxide nanotubes formed over titanium wires, *Environ. Sci. Technol.*, 43 (9) (2009) 3260-3265. https://doi.org/10.1021/es8031049

6. R. Xu, M. Jia, Y. Zhang, F. Li, Sorption of malachite green on vinyl-modified mesoporous poly(acrylic acid)/SiO$_2$ composite nanofiber membranes, *Microporous Mesoporous Mater.,* 149 (2012) 111-118. https://doi.org/10.1016/j.micromeso.2011.08.024

7. J. Labanda, J. Sabaté, J. Llorens, Experimental and modeling study of the adsorption of single and binary dye solutions with an ion-exchange membrane adsorber, *Chem. Eng. J.,* 166 (2011) 536-543. https://doi.org/10.1016/j.cej.2010.11.013

8. M. Zarei, A. Niaei, D. Salari, A.R. Khataee, Removal of four dyes from aqueous medium by the peroxi-coagulation method using carbon nanotube–PTFE cathode and neural network modeling, *J. Electroanal. Chem.*, 639 (2010) 167-174. https://doi.org/10.1016/j.jelechem.2009.12.005

9. C.Z. Liang, S.P. Sun, F.Y. Li, Y.K. Ong, T.S. Chung, Treatment of highly concentrated wastewater containing multiple synthetic dyes by a combined process of coagulation/flocculation and nanofiltration, *J. Membrane Sci.,* 469 (2014) 306-315. https://doi.org/10.1016/j.memsci.2014.06.057

10. Y.C. S. Uma, S. Banerjee, Equilibrium and kinetic studies for removal of malachite green from aqueous solution by a low cost activated carbon, *Ind. Eng. Chem. Res.,* 19 (2013) 1099–1105. https://doi.org/10.1016/j.jiec.2012.11.030

11. T.A. Khan, R. Rahman, I. Ali, E.A. Khan, A.A. Mukhlif, Removal of malachite green from aqueous solution using waste pea shells as low-cost adsorbent–adsorption isotherms and dynamics, *Environ. Toxicol. Chem.,* 96 (4) (2014) 569–578. https://doi.org/10.1080/02772248.2014.969268

12. N. Gupta, A.K. Kushwaha, M.C. Chattopadhyaya, Application of potato (solanum tuberosum) plant wastes for the removal of methylene blue and malachite green dye from aqueous solution, *Arab. J. Chem.,* 9 (2014) S707–S716. https://doi.org/10.1016/j.arabjc.2011.07.021

13. B. Ramaraju, P.M.K. Reddy, C. Subrahmanyam, Low cost adsorbents from agricultural waste for removal of dyes, *Environ. Prog. Sustain. Energy.,* 33 (1) (2014) 38–46. https://doi.org/10.1002/ep.11742

14. A.S. Sartape, A.M. Mandhare, V.V. Jadhav, P.D. Raut, M.A. Anuse, S.S. Kolekar, Removal of malachite green dye from aqueous solution with adsorption technique using Limonia acidissima (wood apple) shell as low cost adsorbent, *Arab J. Chem.,* 10 (2) (2017) S3229-S3238. https://doi.org/10.1016/j.arabjc.2013.12.019

15. T. Santhi, S. Manonmani, V.S. Vasantha, Y.T. Chang, A new alternative adsorbent for the removal of cationic dyes from aqueous solution, *Arab. J. Chem.,* 9 (2016) S466-S474. https://doi.org/10.1016/j.arabjc.2011.06.004

16. V. Muinde, J.M. Onyari, B. Wamalwa, J. Wabomba, R.M. Nthumbi, Adsorption of malachite green from aqueous solutions onto rice husks: kinetic and equilibrium studies, *J. Environ. Prot.,* 8 (2017) 215-230. https://doi.org/10.4236/jep.2017.83017.

17. F. Gündüz, B. Bayrak, Synthesis and performance of pomegranate peel-supported zero-valent iron nanoparticles for adsorption of malachite green, *Desalin. Water Treat.,* 110 (2018) 180–192. https://doi.org/10.5004/dwt.2018.22185

18. K.O. Reddy, C.U. Maheswari, M. Shukla, E. Muzenda, Preparation, chemical composition, characterization, and properties of Napier grass paper sheets, *Sep. Purif. Technol.,* 49 (10) (2014) 1527-1534. https://doi.org/10.1080/01496395.2014.893358

19. V. Sawasdee, N. Pisutpaisal, Feasibility of biogas production from napier grass, *Energy Procedia,* 61 (2014) 1229 – 1233. https://doi.org/10.1016/j.egypro.2014.11.1064

20. Q.L. Lu, L.R. Tang, S. Wang, B. Huang, Y.D. Chen, X.R. Chen, Feasibility of biogas production from napier grass, *Biomass Bioenergy*, 70 (2014) 267-227. https://doi.org/10.1016/j.biombioe.2014.09.012

21. A. Hassani, M. Kiransan, R.D.C. Soltani, A. Khataee, S. Karaca, Optimization of the adsorption of a textile dye onto nanoclay using a central composite design, *Turk. J. Chem.*, 39 (2015) 734-749. https://doi.org/10.3906/kim-1412-64

22. M.H. Baek, C.O. Ijagbemi, S.J. O, D.S. Kim, Removal of malachite green from aqueous solution using degreased coffee bean, *J. Hazard. Mater.*, 176 (2010) 820-828. https://doi.org/10.1016/j.jhazmat.2009.11.110

23. O. Abdi, M. Kazemi, A review study of biosorption of heavy metals and comparison between different biosorbents, *J. Mater. Environ. Sci.,* 6 (5) (2015) 1386-1399. E-mail: abdi.omran@yahoo.com
24. K.O. Reddy, B.R. Guduri, A.V. Rajulu, Structural characterization and tensile properties of borassus fruit fibers, *J. Appl. Polym. Sci.,* 114 (1) (2009) 603-611. https://doi.org/10.1002/app.30584
25. W. Tongpoothorn, M. Sriuttha, P. Homchan, S. Chanthai, C. Ruangviriyachai, Preparation of activated carbon derived from jatropha curcas fruit shell by simple thermo-chemical activation and characterization of their physico-chemical properties, *Chem. Eng. Res. Des.,* 89 (3) (2011) 335-340. https://doi.org/10.1016/j.cherd.2010.06.012
26. X.F. Sun, F. Xu, R.C. Sun, P. Fowler, M.S. Baird, Characteristics of degraded cellulose obtained from steam-exploded wheat straw, *Carbohydr. Res.,* 340 (2005) 97-106. https://doi.org/10.1016/j.carres.2004.10.022
27. I.A.W. Tan, A.L. Ahmad, B.H. Hameed, Optimization of preparation conditions for activated carbons from coconut husk using response surface methodology, *Chem. Eng. J.,* 137 (2008) 462-470. https://doi.org/10.1016/j.cej.2007.04.031
28. G.B. Hong, Y.K. Wang, Synthesis of low-cost adsorbent from rice bran for the removal of reactive dye based on the response surface methodology, *Appl. Surf. Sci.,* 423 (2017) 800-809. https://doi.org/10.1016/j.apsusc.2017.06.264
29. K.K. Bahadir, T. Abdurrahman, Electrochemical treatment of simulated industrial paint wastewater in a continuous tubular reactor, *J. Chem. Eng.,* 148 (2-3) (2008) 444-451. https://doi.org/10.1016/j.cej.2008.09.019
30. I. Arslan-Alaton, G. Tureli, T. Olmez-Hanci, Treatment of azo dye production wastewaters using Photo-Fenton-like advanced oxidation processes: Optimization by response surface methodology, *J. Photoch Photobio A.,* 202(2-3) (2009)142-153. https://doi.org/10.1016/j.jphotochem.2008.11.019
31. M. Karimi, S.A. Milani, H. Abolgashemi, Kinetic and isotherm analyses for thorium (IV) adsorptive removal from aqueous solutions by modified magnetite nanoparticle using response surface methodology (RSM), *J. Nucl. Mater.,* 479 (2016) 174-183. https://doi.org/10.1016/j.jnucmat.2016.07.020
32. M. Saad, H. Tahir , J. Khan, U. Hameed, A. Saud, Synthesis of polyaniline nanoparticles and their application for the removal of Crystal Violet dye by ultrasonicated adsorption process based on response surface methodology, *Ultrason. Sonochem.,* 34 (2017) 600-608. https://doi.org/10.1016/j.ultsonch.2016.06.022
33. Y. Ho, G. McKay, A comparison of chemisorption kinetic models applied to pollutant removal on various sorbents, *Process Saf. Environ.,* 76 (1998) 332-340. https://doi.org/10.1205/095758298529696
34. K.Y. Shin, J.Y. Hong, J. Jang, Heavy metal ion adsorption behavior in nitrogen-doped magnetic carbon nanoparticles: isotherms and kinetic study, *J. Hazard. Mater.,* 190 (2011) 36-44. https://doi.org/10.1016/j.jhazmat.2010.12.102
35. S. Gueu, B. Yao, K. Adouby, G. Ado, Kinetics and thermodynamics study of lead adsorption on to activated carbons from coconut and seed hull of the palm tree, *Int. J. Environ. Sci. Technol.*, 4(1) (2007) 11-17. https://doi.org/10.1007/BF03325956
36. A.W. Ip, J.P. Barford, G. Mckay, Reactive Black dye adsorption/desorption onto different adsorbents: Effect of salt, surface chemistry, pore size and surface area, *J. Colloid Interface Sci.,* 337 (2009) 32–38. https://doi.org/10.1016/j.jcis.2009.05.015
37. I. Langmuir, The adsorption of gases on plane surfaces of glass, mica and platinum, *J. Am. Chem. Soc.,* 40 (1918) 1361-1403. https://doi.org/10.1021/ja02242a004
38. Y. Park, G.A. Ayoko, E. Horváth, R. Kurdi, J. Kristof, R.L. Frost, Structural characterisation and environmental application of organoclays for the removal of phenolic compounds, *J. Colloid Interface Sci.*, 393 (2013a) 319-334. https://doi.org/10.1016/j.jcis.2012.10.067
39. H.M.F. Freundlich, Over the adsorption in solution, *Z. Phys. Chem.,* 57 (1906) 384-470.
40. S. Veli, B. Alyuz, Adsorption of copper and zinc from aqueous solutions by using natural clay, *J. Hazard. Mater.,* 149 (2007) 226-233. https://doi.org/10.1016/j.jhazmat.2007.04.109
41. A.A. Khan, R.P. Singh, Adsorption thermodynamics of carbofuran on Sn (IV) arsenosilicate in H^+, Na^+ and Ca^{2+} forms, *Colloids Surf.,* 24 (1987) 33-42. https://doi.org/10.1016/0166-6622(87)80259-7
42. Y. Sag, T. Kutsal, Determination of the biosorption heats of heavy metal ions on zoogloea ramigera and rhizopus arrhizus, *Biochem. Eng. J.,* 6(2) (2000) 145-151. https://doi.org/10.1016/S1369-703X(00)00083-8

(2019) ; http://www.jmaterenvironsci.com/